Toxicology Research

ARTICLE

Effects of Hydroxyapatite@Poly-Lactide-Co-Glycolide Nanoparticles Combined with Pb and Cd on Liver and Kidney Parenchyma after the Reconstruction of Mandibular Bone Defects

Received 00th January 20xx,
Accepted 00th January 20xx

DOI: 10.1039/C9TX00007K

www.rsc.org/

Nenad L. Ignjatović, [a]* Radmila Janković,[b] Vuk Uskoković,[c] and Dragan P. Uskoković[a]

Reconstruction of bone defects with the use of biomaterials based on hydroxyapatite (HAp) has been a popular approach in medicine and dentistry. Most often the process of new bone formation is analyzed with the focus only on the region of the reconstructed defect. The effects of the therapy on distant organs have been rarely reported in literature, especially not in synergy with the exposure to other bioactive chemicals. In this study, reconstruction of the mandibular bone *in vivo* using poly-lactide-co-glycolide-coated HAp (HAp/PLGA) nanoparticles was monitored with a simultaneous histopathological analysis of distant organs, specifically kidney and liver parenchyma. Heavy metals are among the most prominent environmental pollutants and have a high affinity for the crystal lattice of HAp, where they get incorporated by replacing calcium ions. Lead (Pb) and cadmium (Cd) are two such metals that can be found in food, water and air, but are most commonly present in cigarette smoke, the frequent contaminant of hospital settings in the developing world. The influence of their presence in the repaired bone on the content of calcium (Ca) in the reconstructed bone defect was analyzed, along with the histopathological changes in liver and kidneys. A study performed on 24 female Wistar rats demonstrated that the reconstruction of mandibular bone defects using HAp/PLGA particles induced an increase in the content of Ca in the newly created bone without causing any pathological changes to the liver and the kidneys. The presence of Pb and Cd in the defects reconstructed with HAp/PLGA nanoparticles impeded the regenerative process and led to a severe and irreversible damage to the liver and kidney parenchyma.

Introduction

Calcium phosphates and particularly hydroxyapatite (HAp) as their least soluble phase and the phase bearing most structural resemblance to biogenic apatite have been widely used in reconstructive medicine as materials for the reconstruction of damaged or innately defective bones.[1] HAp has been widely regarded as the epitome of a biocompatible, non-immunogenic and nontoxic biomaterial at all scales: molecular, cellular, organismic.[2] In recent years, the repertoire of applications for HAp-based biomaterials has expanded and they have found an application niche in preventive medicine as molecular imaging agents, but are also used in hyperthermia, photodynamic and radiation therapies.[3] Hybrid systems based on HAp and biocompatible and bioresorbable polymers have been particularly useful in terms of enabling this expansion of the scope of applications for HAp-based biomaterials in reconstructive bone tissue surgery and other fields of bioengineering.[4,5] A particularly prospective complement to HAp in these hybrid systems has been poly-lactide-co-glycolide (PLGA), a biocompatible polymer approved by the Food and Drug Administration (FDA) for use in medical devices.[6]

In a biological environment, degradation of HAp particles is enzymatically controlled and mediated by cells.[7] Phagocytosis of HAp is carried out by osteoclasts and macrophages and ultimately results in its disintegration to elementary ionic units, namely the ions of Ca, phosphate and hydroxyl, which are either excreted or used in different metabolic cycles. Monomeric units of lactic and glycolic acids as the degradation products of PLGA are more structurally complex, but still biocompatible and nontoxic except in rare circumstances[8-10], and are eliminated from the body through normal metabolic pathways, such as the tri-carboxylic acid cycle.[6,11] Because bioresorbable bone replacement materials, including HAp/PLGA, degrade to make way for new bone growth, the focus of a thorough biocompatibility analysis must be not only on bone regeneration alone, but also on the organs potentially affected by these degradation products. At the same time, by the intake of food, water and air, there is always a finite possibility of introducing small amounts of toxic elements that could potentially affect not only the defect reconstruction process, but also the whole organism. Heavy metals are among the biggest environmental pollutants, and contamination with them can be very harmful because of no possibility for biodegradation and because of their cumulative toxic effects. Cadmium (Cd) can often appear as a food and milk contaminant[12,13], while lead (Pb) may be present in drinking water, especially in aged water supply networks.[14,15] Both Cd and Pb are also common ingredients of tobacco smoke[16-18], the frequent third-hand contaminant in hospital settings[19], especially in the developing world.[20] Cd are Pb are often found not only in tobacco smoke, but also in e-cigarettes, where they form in the

[a] *Institute of Technical Sciences, Serbian Academy of Science and Arts, Knez Mihailova 35/IV, P.O. Box 377, 11000 Belgrade, Serbia*
[b] *University of Belgrade, School of Medicine, Institute of Pathology, Belgrade, Serbia*
[c] *University of Illinois, Department of Bioengineering, Chicago, IL, USA*

interaction between hot vapors and the metallic heating coils.[21] Heavy metals, especially Pb, but also Cd, have an affinity for tissues that contain inorganic mineral components, such as boney tissues. There, they replace calcium in the crystal lattice of HAp, causing the loss of bone mass, occurrence of osteoporosis and a change in the structural bone integrity, usually in the direction of accelerated resorptive metabolic processes in the bone.[22-24] Retention and mobility of these metals in boney tissues modifies the function of bone cells, disrupts the metabolism of Ca, thus affecting the production of parathyroid hormone, calcitonin, vitamin D as well as other hormones that affect Ca metabolism.[25] Alongside the affinity for deposition in bones and for causing osteoporosis, Cd and Pb also accumulate in the liver and kidneys.[26,27] These two metals are also cancerous and even a low-level environmental exposure imposes a damaging effect on the cardiovascular system.[28] The metabolic dysfunctions caused by them are commonly manifested as the occurrence of diabetes.[29-31] Pb and Cd also induce tubular osteomalacia, accompanied by hypophosphatemia, hypocalcaemia and osteoporosis.[30]

Notwithstanding the importance of *in vitro* tests, reliable and reproducible *in vivo* assays [32] are a necessary step toward the real-life application of biomaterials in the clinical practice. When it comes to HAp, a biomaterial known for its pleiotropy[33] and ability to elicit both cytocompatible and cytotoxic effects[34], *in vitro* and *in vivo* assays do not necessarily agree in terms of their outcome[35,36], which even further reinforces the necessity for the use of *in vivo* models to assessing their biomedical potentials. Reparation of large bone defects caused by trauma, inflammation or tumor surgery has been performed in the clinic using HAp and analyzed in various animal models, *e.g.* dog, sheep, and goat.[37] The histological analysis of bone reparation with HAp in animal models is one of the most commonly applied techniques for validation of a successful reconstruction process.[38] In our previous study, we demonstrated a successful reconstruction of bone defects with PLGA-coated HAp (HAp/PLGA) nanoparticles and analyzed the reconstructed defect by histopathological and histomorphometric methods.[39] Other studies were performed using the similar approach and the similar material compositions. For example, artificially induced bone defects in animals were reconstructed with a hybrid system combining HAp and polylactide (PLA), and the osteogenic process in the defect was analyzed using infrared spectroscopy.[40] In another study, the possibility of using HAp and PLA-based systems in the orbital wall fracture reconstruction was assessed in 70 human subjects, and reconstructions were analyzed by means of computerized tomography.[41] Likewise, femoral radiographs of a dog bone defect were analyzed before and after the reconstruction of the defect with a HAp and PLA composite material.[42] An HAp/PLA system was also used for the internal fixation of bone fractures and the fixation performance was analyzed for 7 years by scanning electron microscopy (SEM).[43,44] A histopathological analysis of animal bone defects reconstructed with the use of nano-HAp coated with poly-lactide-co-glycolide (PLGA) and chitosan (Ch) particles was also performed in an effort to elucidate the effects of one such multipolymeric system on bone regeneration. Common to all these analyses was the assessment of the quality of the newly formed tissue in the defect only, while marking down the overall morbidity, yet without monitoring the histopathological effects on other organs.[45]

In this study, we attempt to go beyond this approach and focus not only on the very defect and its immediate surroundings, but also on the effects of reconstruction on two distant organs of choice: liver and kidneys. Specifically, we demonstrate the reconstruction of the mandibular bone defect in female Wistar rats using HAp/PLGA and analyze the contents of calcium (Ca) in the reconstructed defect. Ca content is essential for the differentiation of progenitor and hematopoietic stem cells into osteogenic and osteoclastic phenotypes that form the new bone through mutual functional orchestration.[46] At the same time, histopathological methods were used to determine whether the biodegraded products of the implant integration process affect organs distant to the reconstructed defect, namely kidneys and liver. The influence of the presence of Pb and Cd on Ca content in the reconstructed bone defects as well as on these two distant organs was analyzed within 6 - 12 weeks of post-implantation time. The two heavy elements were administered simultaneously, given that earlier studies have shown that even when elevated concentrations of Pb and Cd alone produce no adverse health effects, their synergy does.[47]

Experimental

Synthesis of HAp/PLGA particles

Aqueous calcium nitrate ($Ca(NO_3)_2$) solution (150 ml; 26.6 wt. %) was added to the solution of ammonium phosphate ($(NH_4)_3PO_4$) (7 ml H_3PO_4+165 ml NH_4OH+228 ml H_2O) at 50 °C over the period of 60 minutes, while stirring at the rate of 100 rpm. The solution was then brought to the boiling point and maintained there for 60 minutes.[39] The resulting gel was dried at room temperature in a vacuum drier for 72 h, after which the product - HAp particles – was obtained. Poly-DL-lactide-co-glycolide (PLGA) (50:50) (Sigma Chemical Company, USA) was used as the polymer component. HAp/poly-DL-lactide-co-glycolide (HAp/PLGA) particles were synthesized by the emulsion procedure using a solvent–non-solvent system.[39,48] The particles of HAp were added to a completely dissolved polymeric solution to the concentration of 80 wt.%. The suspension was mixed at the velocity of 1000 rpm, at which point methanol was added to the mixture. Afterwards, PVA (0.02% in water) was added to the suspension (PLGA/PVA = 10/1). After the solvent had evaporated in the vacuum drying oven at 20 °C and 1 Pa for 6h, the particles were dried at room temperature for 24 h. The resulting powder was washed with distilled water three times, centrifuged at 1000 rpm and dried again, after which the final product was obtained in the form of HAp/PLGA particles with the weight ratio of HAp : PLGA of 80 : 20. The encapsulation efficiency was 94%. The particles of the HAp/PLGA were sterilized by γ-rays (25 kGy) before use.

Characterization of the products

X-Ray diffraction (XRD) was performed on a Philips PW-1050 diffractometer with Ni-filtered $Cu_{K\alpha}$ radiation and the scanning step of 0.02°. The particle size distribution (PSD) was measured on 10 mg/ml of powders dispersed in water using a Mastersizer 2000 (Malvern Instruments Ltd.) and a *HydroS* dispersion unit for liquid dispersants. Water was selected as the dispersion medium in order to reduce the charge screening effect present at the higher ionic strength in physiological media and thus minimize particle aggregation. Fourier-transform infrared spectroscopy (FT-IR) was done on a Nicolet iS10 FT-IR Spectrometer (Thermo Scientific Instruments) in the spectral range from 400 to 4000 cm^{-1}. Morphological analysis was performed using a SUPRA 35 VP Carl Zeiss field emission scanning electron microscope (SEM). Electrokinetic parameters of the suspensions of synthesized

particles were analyzed using a Zeta-Sizer Nano (Malvern Instruments Ltd.) in distilled water and pH 6.5.

***In vivo* experiments**

The procedures involving experimental animals were done in compliance with the Guidelines for Work with Experimental Animals adopted by the Ethical Committee of the Faculty of Medicine, University of Niš, Serbia. The experiments were performed on white female rats of the Wistar strain aged 6–8 weeks, of an average weight of 200 g. Animals were raised in the laboratory, with a standard diurnal and feeding regimen. Animals were divided into two groups: 1) Experimental group (A - 16 animals); 2) Control group (B - 8 animals).

In the experimental group of animals, a bone defect 1.4 mm in diameter and 1.6 mm in depth in the region between the medial line and the foramen mentale on the left side of the mandible was induced using a sterile steel borer. HAp/PLGA particles were implanted in the mandible defect. The animals belonging to the experimental group were further divided into three subgroups: A1 - HAp/PLGA particles in the paste form, obtained by mixing HAp/PLGA powder with physiological saline; A2 - HAp/PLGA powder mixed with a dilute aqueous solution of $PbCl_2$ and $CdCl_2$, the concentration of which was adjusted to 5 μg of Pb and 5 μg of Cd per gram of the rat's body weight in total; A3 - HAp/PLGA powder mixed with a concentrated solution of Pb and Cd, using the same chloride salts, the concentration of which was adjusted to 50 μg of Pb and 50 μg Cd per gram of the rat's body weight in total. Compositions of the three sample groups are summed in Table 1.

Tab. 1 Sample group names and compositions. Units for [Pb] and [Cd] represent the amount of the chemical element per the rat's body weight.

Sample	HAp/PLGA	[Pb] (μg/g)	[Cd] (μg/g)
A1	Yes	0	0
A2	Yes	5	5
A3	Yes	50	50
B	No	0	0

In the Control group (B), the regular diurnal and feeding regimen was maintained, and these animals received no therapy. The animals in all four sample groups (A1, A2, A3, and B) were sacrificed 6 and 12 weeks after the implantation. A bone sample was obtained from the region between the medial line and the foramen mentale on the left side of the mandible, where the implantation was performed. Jawbone samples from all four sample groups were treated in the mixture of 5ml HNO_3 (67%) and 7mL HCl (37%) in order to degrade the organic tissue. The mixtures were gradually heated until the temperature of 130°C was reached. That temperature was maintained during the mineralization period (for two hours). After the cooling, 3 x 15 ml of bi-distilled water was added to each of the solutions. Solutions were then evaporated until the 1-2 ml volume was reached. The solutions with sediments were filtered through the Whatman No. 541 filter paper, and the filtrates were dissolved in 250 ml of de-ionized water. In these solutions, the total concentration of Ca was determined. Ca was measured by means of atomic absorption spectrophotometric analysis (AAS, Perkin-Elmer M 1100). Bone tissue samples were kept in physiological saline, to be subsequently dried until a constant mass was reached, grinded and divided into defined aliquots, and dissolved in 67% HNO_3 at 25-30°C. Then 37% HCl was added and steamed until the dry mass was reached, so that the remaining nitrogen compounds could be disposed of. By eliminating unfavorable effects of nitrates, cations can be translated into chloride compounds, which allow for effective detection of inorganic components by AAS. For that reason the bone samples were dissolved in deionized water until defined aliquots, suitable for detection via AAS, were reached. Soft tissue samples (kidney and liver) were formalin-fixed and paraffin-embedded for histopathological evaluation. Histological sections were stained using hematoxylin–eosin (H&E) and periodic acid–Schiff (PAS) methods.

Results and discussion

Fig. 1 shows the results of the basic physicochemical characterization of the synthesized HAp and HAp/PLGA powders. The XRD patterns of HAp and HAp/PLGA (Fig. 1a) confirmed a poorly crystalline structure of HAp, typical for precipitation under ambient conditions and practically any method that circumvents high-temperature processing of this compound. Expectedly, no peaks corresponding to PLGA were detected in the diffractogram because this polymer is amorphous.[49] The FT-IR spectra of HAp and HAp/PLGA are presented in Fig. 1b. They are both dominated by a doublet with maxima at ~1050 and ~1090 cm^{-1}, which originate from the ν_3 antisymmetric stretching mode of the phosphate group. Another prominent band originating from a phosphate group vibration is the doublet with maxima at somewhat lower frequencies of ~ 570 and ~ 600 cm^{-1}, arising from the ν_4 triply degenerated bending mode of the phosphate tetrahedron. The absorption maximum at ~3560 cm^{-1} originates from the stretch of the OH^- group, while the relatively intense and sharp band at ~1760 cm^{-1} is attributed to the C=O vibration from PLGA.[48] The particle size distributions in HAp and HAp/PLGA powders are shown in Fig. 1c. The average mass diameter, d_{50}, corresponding to a value that has 50% of the particles smaller than it and 50 % larger than it, amounted to 70 nm for HAp, and 82 nm for HAp/PLGA. With d_{10} = 47 nm, d_{50} = 82 nm and d_{90} = 183 nm, the majority of HAp/PLGA particles were nanosized in nature, having less than 100 nm in diameter. The measured polydispersion index (PDI) for HAp/PLGA particles equalled 0.63. Figure 1d shows the morphology of primary particle units within larger agglomerates in dried HAp/PLGA powder. The basic spherical nanoparticles of HAp/PLGA joined together into bigger agglomerates by adhesive forces.

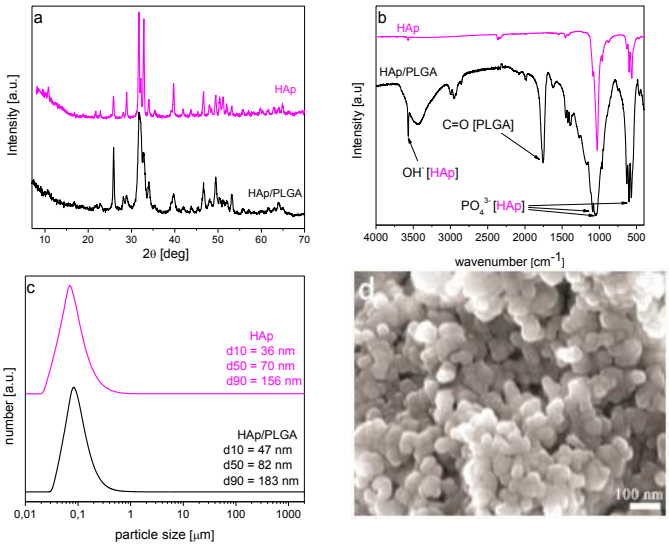

Fig. 1 Results of the physicochemical characterization of HAp and HAp/PLGA powder: a) X-ray diffraction pattern, b) FT-IR spectrum, c) particle size distribution, and d) an SEM image of dry HAp/PLGA powder.

Zeta potential (ZP) values at pH 6.5 equalled -7.5 ± 0.5 mV for HAp and -22.1 ± 0.9 mV for HAp/PLGA. Generally, ZP values within the 0 to ± 15 mV range indicate sols prone to flocculation and aggregation, whereas absolute ZP values higher than 15 mV are characteristic for stable and aggregation-resistant particles.[50] Considering the ZP values for HAp (< 15 mv on the absolute scale) and HAp/PLGA (> 15 mV on the absolute scale), it can be concluded that the addition of PLGA increases the stability of HAp particles in the conditions where surface charge is its main determinant. The increased negative charge of the particles resulting from the addition of PLGA can be ascribed to the dissociation of carboxylic terminal groups and the formation of negatively charged COO^- residues on the particle surface.

The results presented in Fig. 2 show that the implantation of the A1 subgroup of HAp/PLGA nanoparticles, containing neither Pb nor Cd, led to an increase in the amount of Ca per weight of the reconstructed alveolar bone sample by 6.3 % after 6 weeks and by 10.7 % after 12 weeks, at which point the increase was statistically significant compared to the control B. Ca analysis of bone samples from the A2 and A3 subgroups, where the solutions of Pb and Cd were mixed in to the implanted paste, showed a reduced bone tissue formation compared to both the negative control B and the A1 subgroup, which contained neither Pb nor Cd. Compared to the control B, the treatment with the diluted solution of Cd and Pb (A2) caused a 2.7 % loss of Ca per weight of the reconstructed alveolar bone after 6 weeks and a 6.4 % loss after 12 weeks. The Ca loss effect was even more significant in animals treated with the A3 subgroup, containing ten times higher concentration of Pb and Cd compared to the A2 subgroup. Specifically, animals in the A3 subgroup exhibited a 5.1 % decrease in the amount of Ca in the alveolar bone after 6 weeks and a 10.8 % decrease after 12 weeks compared to the control B, at which point the effect was statistically significant compared to A2. These results demonstrate that pure HAp/PLGA nanoparticles, uncontaminated with Pb and Cd, promoted regeneration of the alveolar bone. This positive effect, however, becomes annulled when Pb and Cd are added even at comparatively low concentrations to HAp/PLGA 6 weeks after the implantation and becomes significantly deleterious 12 weeks after the implantation. Higher concentrations of Pb and Cd had an even more pronounced effect on reduced bone regeneration with the use of HAp/PLGA nanoparticles, in which case the effect was statistically significant in comparison to the control already after 6 weeks. Therefore, the detrimental effect of adding Pb and Cd to HAp/PLGA implants was present even at the lowest tested concentration of 5 μg x g^{-1} when normalized to the animal body weight; it was pronounced both with respect to the bone treated with the use HAp/PLGA and the control bone; finally, it increased with the concentration of Pb and Cd contaminants and was cumulative, becoming more pronounced at longer post-implantation times.

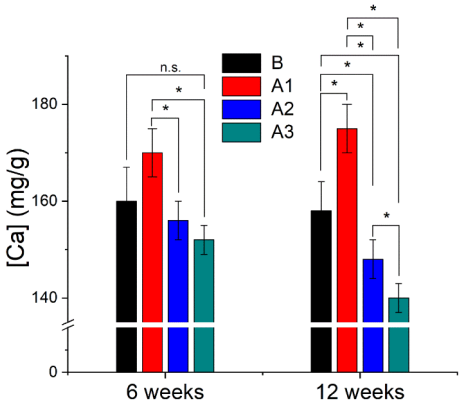

Fig. 2 Amount of Ca per the weight of the reconstructed alveolar bone of the rats 6 and 12 weeks after the implantation of the HAp/PLGA nanoparticles. Data points are shown as averages and error bars represent standard deviation. Statistically significant difference between sample subgroups ($p < 0.05$) is denoted with *. Difference between subgroups that are either not connected with an asterisk or connected with n.s. is not statistically significant ($p > 0.05$).

The effects of Pb and Cd exhibited directly on the newly grown bone are caused by the toxicity of these ions imposed on cells populating the bone, but also by the weakening of the bone mineral entailed by the replacement of Ca in apatite crystals by Pb and Cd cations having the same valence state as Ca (+2). The ionic radii of Pb (133 pm) and Cd (109 pm) differ from the radius of the Ca ion (114 pm) and while Pb cation is considerably larger than Ca, Cd is somewhat smaller than it. Their substitution for Ca (Fig.3) is thus bound to have mutually opposite effects on the lattice of apatite: while Cd will shrink it locally, Pb will expand it and the cumulative effect will depend on the ratio between the concentrations of the two dopants in the solid phase. Because Cd is more similar in size to Ca, which it substitutes for, and Pb is significantly larger, it is possible that Cd would accommodate itself more efficiently, while Pb may even precipitate as a separate phase, in which case lattice contraction could be expected. A recent study demonstrated an effect of Pb on altering gene expression in osteoblasts, but also showed its close association with the bone mineral, where it localized with Ca, but also formed a separate phase.[51] Concurrent adsorption of Cd and Pb on HAp confirmed the formation of a separate precipitate containing Pb and retention of the structure and morphology of HAp upon the sorption of Cd.[52] Other adsorption studies on pure HAp have shown excellent capture and immobilization of both of these ions agreeing [53-55] with the earlier established premise that the majority of Periodic Table elements could be accommodated stably inside the lattice of HAp.[56] Even though no charge imbalance is introduced to the lattice with Ca → Pb/Cd substitution because both Pb and Cd are divalent, like Ca, their accommodation will alter the bond angles at the unit cell scale and reduce the long-range crystalline symmetry, which is in apatite manifested as increased solubility and resorption rate. It should also be added that although this ion substitution effect is detrimental to the mechanical properties of apatite, it may mitigate some of the adverse effect Pb and Cd impose on cells and soft tissues by sequestering these toxic ions. Co-administrations of nano-HAp and Cd/Pb, for example, has been capable of mitigating the toxic effects of the latter ions.[57-59]

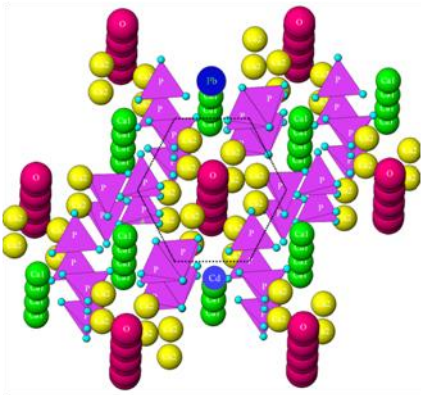

Fig. 3 One smaller Cd^{2+} ion and one larger Pb^{2+} ion substituting for a columnar, Ca1 cation each in the crystal structure of HAp. This ionic size difference causes distortions in bond angles and lengths, reducing the overall crystallinity and promoting bioresorption. The hexagonal center of symmetry is depicted with a dashed line. Different ionic elements are represented with different colors: columnar, Ca1 calcium in green, hexagonal, Ca2 calcium in yellow, hydroxyl in magenta, phosphate in purple, Cd in light blue and Pb in dark blue.

To inspect whether the observed changes in the amounts of Ca per the weight of the alveolar bone, indicative of the quality of the regenerated bone, corresponded to the changes in the liver and the kidneys, these two remote organs were subjected to a histological analysis, the results of which are shown in Figs. 4-7. Kidney (Fig.4a) and liver (Fig.4b) parenchyma of the control group, B, showed a perfectly normal histological structure, without any pathological changes. No changes were detected in the control group for either time interval (6 and 12 weeks). In animals subjected to the treatment with the A1 sample subgroup, i.e. HAp/PLGA nanoparticles without any exposure to Pb or Cd, the kidney tissue samples showed a slight stasis (arrows) in the medulla 6 weeks after the implantation (Fig. 5a). Stasis was more pronounced (arrow), with slightly dilated lumens of glomerular capillaries (arrowhead), 12 weeks after the procedure (Fig. 5b). Meanwhile, the proximal tubule epithelium was intact, with no cylinders in the lumen, and the interstitial appeared slightly expanded. The parenchyma of the liver showed a slight dilatation of blood vessels (arrow) 6 weeks after the implantation of HAp/PLGA nanoparticles from the same subgroup A1 (Fig. 5c), whereas after 12 weeks moderate venostasis was present (arrows) (Fig. 5d). No other pathological changes were observed. The initial signs of stasis without pathological changes are expected to have been the result of the experimental conditions in which the animals lived.

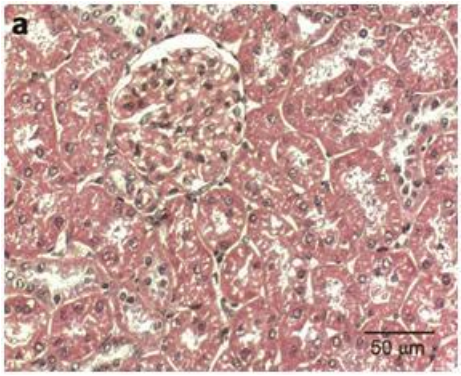

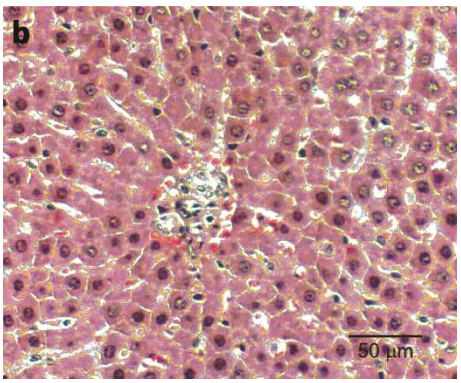

Fig. 4 Control group (B) showing no histopathological changes: a) kidney, b) liver *(HE x 20).*

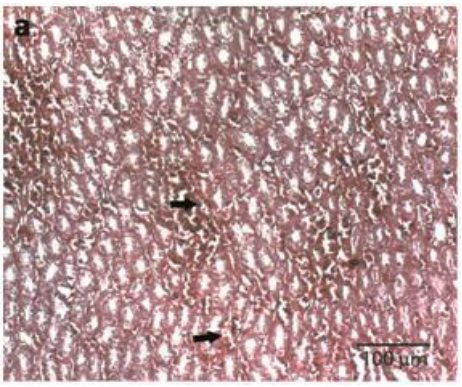

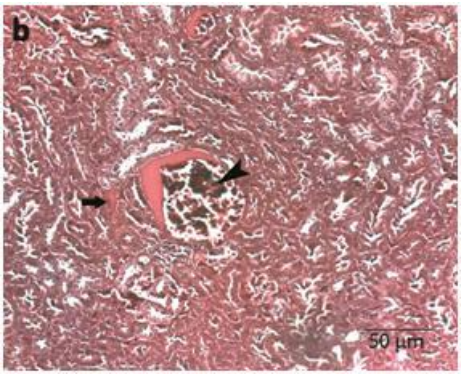

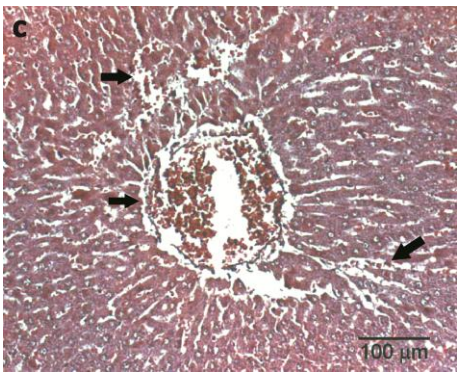

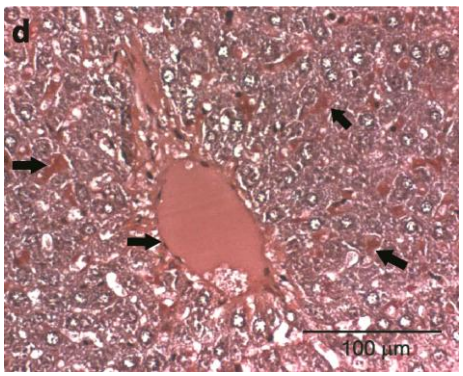

Fig. 5 Histopathological changes in the parenchymatous organs of animals in the experimental subgroup A1: a) kidneys after 6 weeks, b) kidneys after 12 weeks, c) liver after 6 weeks, d) liver after 12 weeks. *(HE x 20)*

In animals subjected to the treatment with the A2 sample subgroup, i.e. HAp/PLGA nanoparticles combined with the lower of the two tested concentrations of Pb and Cd, the kidneys, apart from stasis, displayed clear signs of degeneration in the tubular epithelium, such as scattered desquamation of epithelial cells into the lumen (arrows), six weeks after the implantation (Fig. 6a). Changes were more prominent 12 weeks after the procedure, at which point the examined kidney tissue showed a massive dilatation of capillary lumens (arrows), with the extreme narrowing of capsular spaces (arrowheads) (Fig. 6b). Epithelial desquamation in the lumen was also noticed, along with the slight dilatation of the interstitial blood vessels. The described changes were consistent with the stasis in the kidney parenchyma. Apart from the pronounced stasis, clear signs of tubular degeneration could be seen and the lumens of both small and large blood vessels were dilated. Six weeks after the implantation of HAp/PLGA nanoparticles mixed with the dilute solution of Pb and Cd into the alveolar bone of the rats, the liver tissue also exhibited signs of stasis, alongside the destruction of liver plates as well as the vacuolar degeneration of hepatocytes (arrows) and the blood vessel dilatation (arrowheads) (Fig. 6c). Dilatation of the blood vessels (arrowheads) and changes induced by stasis were more pronounced after 12 weeks and accompanied with the degradation of the liver plates and the vacuolar degeneration of hepatocytes (arrows) (Fig. 6d). Other pathological changes were not observed.

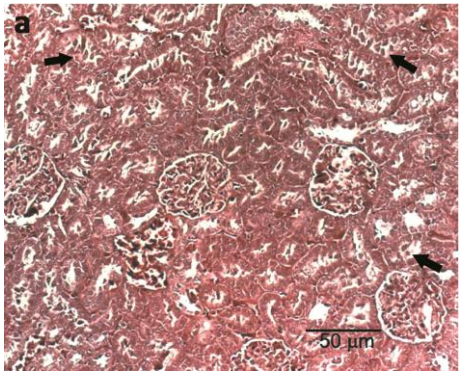

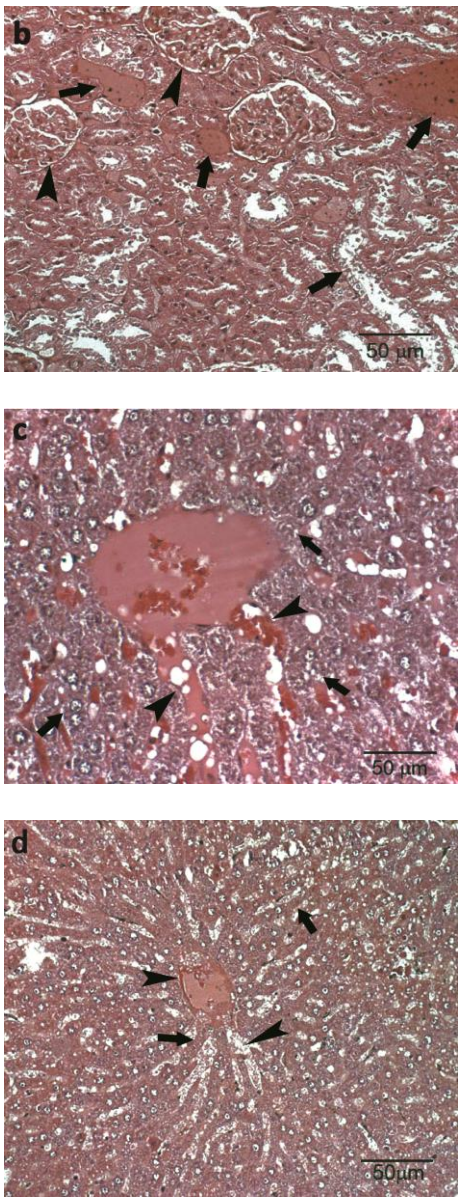

Fig. 6 Histopathological changes in the parenchymatous organs of animals in the experimental subgroup A2: a) kidneys after 6 weeks, b) kidneys after 12 weeks, c) liver after 6 weeks, d) liver after 12 weeks. *(HE x 20)*

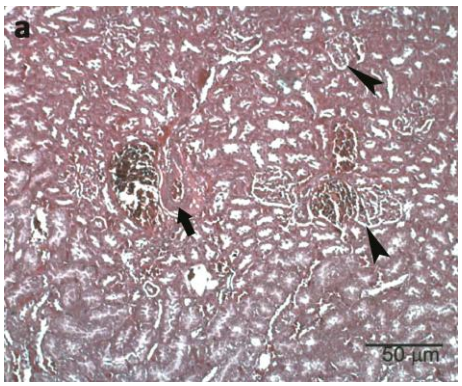

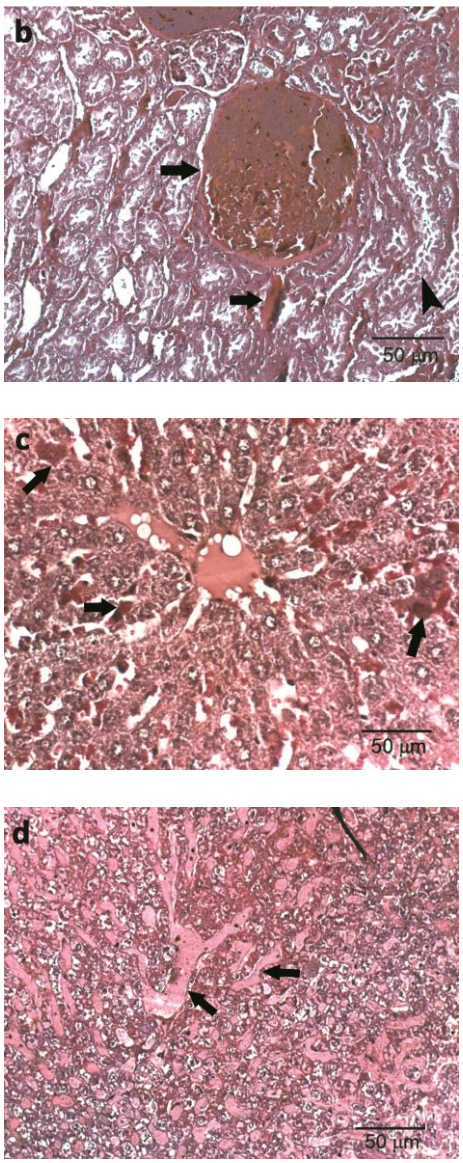

Fig. 7 Histopathological changes in the parenchymatous organs of animals in the experimental group A3: a) kidneys after 6 weeks, b) kidneys after 12 weeks, c) liver after 6 weeks, d) liver after 12 weeks. *(HE x 20)*

Six weeks after the implantation of A3 sample subgroup, *i.e.* HAp/PLGA nanoparticles combined with the higher of the two tested concentrations of Pb and Cd, into the alveolar bone of the rat, clear changes in the parenchyma of the kidneys were observed. Specifically, capsular spaces narrowed (arrowheads) and glomerular capillaries showed signs of dilatation. Larger arteries and veins were extremely dilated and filled with erythrocytes (arrow) (Fig. 7a). Twelve weeks after the intervention, the present glomeruli showed major changes caused by stasis, such as the dilatation of capillary lumens filled with erythrocytes (arrows) and thrombosis in some capillary lumens. The proximal convoluted tubules also displayed epithelial necrosis (arrowhead) (Fig. 7b). Six weeks after the implantation of HAp/PLGA nanoparticles mixed with the high concentration of Cd and Pb, severe degeneration and necrosis of hepatocytes (arrows) could be observed in the liver (Fig. 7c). Twelve weeks after the intervention, the liver parenchyma exhibited severe structural deformation of the hepatic plates, while hepatocytes showed signs of hydropic and vacuolar degeneration. The wall of vena centralis thickened, without sinusoidal fibrosis or cellular infiltration. The pronounced stasis was presents in other parts of the parenchyma too (arrows) (Fig. 7d).

These toxic effects on distal tissue morphologies were detected at both the higher and the lower end of the 5 – 50 µg/g of the animal body weight range chosen for the concentration of the two heavy metals, Pb and Cd. Chronic toxicity for Pb and Cd occurs at the blood levels of circa 0.5 µg/ml and 0.05 µg/ml, respectively.[60,61] Given that the release of these ions from the bone implants will be sustained, paralleling the implant resorption, which lasts for longer than 12 weeks, the blood concentrations in the animals must have been markedly lower than the levels leading to chronic toxicity. Also, animal models of acute exposure to Cd and Pb have used the orally administered concentrations of 15 and 150 µg/g of the body weight in Wistar rats, respectively[62], which correspond to higher heavy metal concentrations than attainable in our model. The fact that definite toxic effects were detectable in distal organs following the implantation of Pb- and Cd-contaminated HAp/PLGA particles shows that even relatively low levels of exposure to these two elements combined with surgical bone graft implantation are not to be dismissed, given that they can elicit a considerable toxic response. The concentrations of heavy metals used in this study were, however, circa 500 times higher than those found in an average cigarette[63] and it would be interesting to explore the toxicity even at these finer doses resulting from the hypothetical exposure of implants to the cigarette smoke.

Overall, the results of this *in vivo* study show that Cd and Pb, finding way to the bone void and/or the implant filling it, decrease the reparatory impact of the filler, in this case HAp/PLGA nanoparticles. Implanted into the alveolar bone of experimental animals, these nanoparticles significantly improve the bone regeneration rate compared to the no-treatment group, but only if the exposure to Pb and Cd is avoided. When the treatment with HAp/PLGA was coupled to the exposure to Pb and Cd, the treatment was detrimental to the healed bone and to the remote organs in the experimental animals. Comparing the outcomes of the treatment 6 and 12 weeks after the implantation at the same concentration of Pb and Cd, a significantly lower bone mass and the quality of the reconstructed bone can be deduced from the lower Ca content in bone at longer post-implantation times (12 weeks < 6 weeks) and also at higher heavy ion doses (A3 < A2) in Pb- and Cd-containing HAp/PLGA sample groups, A2 and A3 (Fig. 2). A more pronounced difference in the bone mass between the control and the experimental groups observed 12 weeks after the implantation than 6 weeks after it was due to the time-dependent accumulation of Pb and Cd in tissues. These metals tend to accumulate in calcified tissues[64,65] and this accumulation coincides with the reduction in the concentration of Ca in bone, which, in turn, leads to a reduction in the mechanical resilience of the bone. Cd, for example, induces bone loss and creates osteoporotic symptoms in bone following environmental levels of exposure[66], while Pb equally reduces the bone Ca content[67], similar to the effects observed in this study (Fig. 2). Human populations thriving on land polluted with unsafe levels of Cd are known to be at a higher risk for bone fracture[68,69] but also renal dysfunction.[70] Prolonged exposure to low levels of Cd is known to cause histological changes in certain parenchymatous organs, especially kidneys, liver, lungs, nasal mucosa, etc.[71,72] and is in agreement with the similar histopathological changes observed in kidneys and liver of animals challenged here with Cd and Pb. These metals are extremely motile and easily distributable to remote tissues through the bloodstream.[73,74] As demonstrated by this study, their effects on organs distant from the region of bone subjected to the surgical treatment are pronounced.

Conclusions

Here we report on the simultaneous evaluation of the effect of a hybrid biomaterial systems composed of HAp nanoparticles coated by the bioresorbable polymer, PLGA, on the quality of bone tissue reconstruction and the quality of tissues and organs potentially influenced by the degradation products generated during and after the reconstruction. The obtained results show that the implantation of HAp/PLGA particles into the alveolar bone of experimental animals increases the mass of Ca in bones, without pathological changes in the liver and the kidneys. This effect is more pronounced after longer periods of time following the implantation of the nanoparticles. Both low and high concentrations of Pb and Cd added to HAp/PLGA nanoparticles decrease their regenerative impact, whereas the effect of the higher concentrations of these toxic elements is more pronounced than that of the lower ones. This can be explained by the tendency of the heavy metals to deposit in calcified tissues, where their concentration rises over time, causing the reduction in the concentration of Ca, along with the mechanical weakening of jawbones. The transport of Pb and Cd from the implantation site to distant tissues and organs, such as liver and kidneys, via bodily fluids caused a severe irreversible damage to these parenchymatous organs. The cumulative effect of Pb and Cd, particularly apparent 12 weeks after the implantation, induced significant histopathological changes to the mentioned organs, including severe stasis. Apart from it, degeneration and necrosis of the tubular epithelium was also noticed. Glomeruli displayed morphological changes caused by the stasis, such as the dilatation of capillary lumens, erythrocyte overflow and thrombosis in numerous capillaries. Some of the blood vessels were affected by parietal thrombosis too. Hepatocytes, in turn, exhibited severe vacuolar, hydropic, degenerative and necrotic changes, with a drastic destruction of liver plates accompanied by prominent venostasis. These results suggest that exposures to heavy metals as environmental or procedural contaminants should be carefully monitored, for their effect on the success of an otherwise immaculate therapy can be immense. Synergies of this type, involving the combination of a tissue regeneration approach and exposure to an adverse environmental chemical, should be paid close attention to in the process of designing appropriate reconstructive therapies.

Conflicts of interest

There are no conflicts of interest to declare.

Acknowledgements

Research presented in this article was supported by the Ministry of Education, Science and Technological Development of the Republic of Serbia (project No. III45004). The authors would also like to thank late Drs. Zorica Ajduković and Vojin Savić of the Medical School at the University of Niš for the performance of *in vivo* experiments and to dedicate this paper to their memory.

References

1 W. Habraken, P. Habibovic, M. Epple and M. Bohner, *Mater. Today*, 2016, **19**, 69–87.
2 N. S. Remya, S. Syama, V. Gayathri, H. K. Varma and P. V. Mohanan, *Colloids Surfaces B Biointerfaces*, 2014, **117**, 389–397.
3 C. Qi, J. Lin, L. H. Fu and P. Huang, *Chem. Soc. Rev.*, 2018, **47**, 357–403.
4 S. V. Dorozhkin, *J. Mater. Sci.*, 2009, **44**, 2343–2387.
5 N. Ramesh, S. C. Moratti and G. J. Dias, *J. Biomed. Mater. Res. - Part B Appl. Biomater.*, 2018, **106**, 2046–2057.
6 P. Gentile, V. Chiono, I. Carmagnola and P. V. Hatton, *Int. J. Mol. Sci.*, 2014, **15**, 3640–3659.
7 Z. Sheikh, M. N. Abdallah, A. A. Hanafi, S. Misbahuddin, H. Rashid and M. Glogauer, *Materials (Basel).*, 2015, **8**, 7913–7925.
8 E. Solheim, B. Sudmann, G. Bang and E. Sudmann, *J. Biomed. Mater. Res.*, 2000, **49**, 257–263.
9 J. Tiainen, Y. Soini, E. Suokas, M. Veiranto, P. Törmälä, T. Waris and N. Ashammakhi, *J. Mater. Sci. Mater. Med.*, 2006, **17**, 1315–1322.
10 A. Plachokova, D. Link, J. van den Dolder, J. van den Beucken and J. Jansen, *J. Tissue Eng. Regen. Med.*, 2007, **1**, 457–464.
11 H. K. Makadia and S. J. Siegel, *Polymers (Basel).*, 2011, **3**, 1377–1397.
12 T. H. Le, I. Alassane-Kpembi, I. P. Oswald and P. Pinton, *Sci. Total Environ.*, 2018, **622–623**, 841–848.
13 P. G. Reeves and R. L. Chaney, *Sci. Total Environ.*, 2008, **398**, 13–19.
14 P. Jarvis, K. Quy, J. Macadam, M. Edwards and M. Smith, *Sci. Total Environ.*, 2018, **644**, 1346–1356.
15 D. Q. Ng, C. Y. Chen and Y. P. Lin, *Sci. Total Environ.*, 2018, **637–638**, 1423–1431.
16 D. Bernhard, A. Rossmann and G. Wick, *IUBMB Life*, 2005, **57**, 805–809.
17 P. Richter, O. Faroon and R. S. Pappas, *Int. J. Environ. Res. Public Health*, 2017, **14**, 1154.
18 K. Ganguly, B. Levänen, L. Palmberg, A. Åkesson and A. Lindén, *Eur. Respir. Rev.*, 2018, **27**, 170122.
19 T. F. Northrup, A. M. Khan, P. Jacob, N. L. Benowitz, E. Hoh, M. F. Hovell, G. E. Matt and A. L. Stotts, *Tob. Control*, 2016, **25**, 619–623.
20 K. Rijhwani, V. R. Mohanty, A. Y. Balappanavar and S. Hashmi, *Asian Pac. J. Cancer Prev.*, **19**, 2097–2102.
21 P. Olmedo, W. Goessler, S. Tanda, M. Grau-Perez, S. Jarmul, A. Aherrera, R. Chen, M. Hilpert, J. E. Cohen, A. Navas-Acien and A. M. Rule, *Environ. Health Perspect.*, 2018, **126**, 027010.
22 Astdr, in *ATSDR's Toxicological Profiles*, 2002, pp. 121–189.
23 E. K. Vig and H. Hu, *J. Am. Geriatr. Soc.*, 2000, **48**, 1501–6.
24 X. Chen, S. Ren, G. Zhu, Z. Wang and X. Wen, *Environ. Toxicol. Pharmacol.*, 2017, **54**, 162–168.
25 J. G. Pounds, G. J. Long and J. F. Rosen, in *Environmental Health Perspectives*, 1991, vol. 91, pp. 17–32.
26 A. Rani, A. Kumar, A. Lal and M. Pant, *Int. J. Environ. Health Res.*, 2014, **24**, 378–399.
27 M. Wallin, L. Barregard, G. Sallsten, T. Lundh, M. K. Karlsson, M. Lorentzon, C. Ohlsson and D. Mellström, *J. Bone Miner. Res.*, 2016, **31**, 732–741.
28 B. P. Lanphear, S. Rauch, P. Auinger, R. W. Allen and R. W. Hornung, *Lancet Public Heal.*, 2018, **3**, e177–e184.
29 J. I. Kuriwaki, M. Nishijo, R. Honda, K. Tawara, H. Nakagawa, E. Hori and H. Nishijo, *Toxicol. Lett.*, 2005, **156**, 369–376.
30 S. Satarug, M. Nishijo, J. M. Lasker, R. J. Edwards and M. R. Moore, *Tohoku J. Exp. Med.*, 2006, **208**, 179–202.
31 M. Wu, J. Song, C. Zhu, Y. Wang, X. Yin, G. Huang, K. Zhao,

J. Zhu, Z. Duan and L. Su, *Oncotarget*, 2017, **8**, 113129–113141.
32 M. M. Stevens, R. P. Marini, D. Schaefer, J. Aronson, R. Langer and V. P. Shastri, *Proc. Natl. Acad. Sci.*, 2005, **102**, 11450–11455.
33 V. Uskoković, *RSC Adv.*, 2015, **5**, 36614–36633.
34 M. P. Masouleh, V. Hosseini, M. Pourhaghgouy and M. K. Bakht, *Curr. Pharm. Des.*, 2017, **23**, 2930-2951.
35 N. Ignjatović, Z. Ajduković, V. Savić, S. Najman, D. Mihailović, P. Vasiljević, Z. Stojanović, V. Uskoković and D. Uskoković, *J. Mater. Sci. Mater. Med.*, 2013, **24**, 343–354.
36 N. Ignjatović, V. Uskoković, Z. Ajduković and D. Uskoković, *Mater. Sci. Eng. C*, 2013, **33**, 943–950.
37 R. Cancedda, P. Giannoni and M. Mastrogiacomo, *Biomaterials*, 2007, **28**, 4240–4250.
38 H. L. Oliveira, W. L. O. Da Rosa, C. E. Cuevas-Suárez, N. L. V. Carreño, A. F. da Silva, T. N. Guim, O. A. Dellagostin and E. Piva, *Calcif. Tissue Int.*, 2017, **101**, 341–354.
39 N. L. Ignjatovic, Z. R. Ajdukovic, V. P. Savic and D. P. Uskokovic, *J. Biomed. Mater. Res. - Part B Appl. Biomater.*, 2010, **94**, 108–117.
40 N. Ignjatović, V. Savić, S. Najman, M. Plavšić and D. Uskoković, *Biomaterials*, 2001, **22**, 571–575.
41 K. Kohyama, Y. Morishima, K. Arisawa, Y. Arisawa and H. Kato, *J. Plast. Reconstr. Aesthetic Surg.*, 2018, **71**, 1069–1075.
42 T. T. Nguyen, T. Hoang, V. M. Can, A. S. Ho, S. H. Nguyen, T. T. T. Nguyen, T. N. Pham, T. P. Nguyen, T. L. H. Nguyen and M. T. D. Thi, *Adv. Nat. Sci. Nanosci. Nanotechnol.*, 2017, **8**, 045013.
43 T. Furukawa, Y. Matsusue, T. Yasunaga, Y. Shikinami, M. Okuno and T. Nakamura, *Biomaterials*, 2000, **21**, 889–898.
44 S. Hasegawa, S. Ishii, J. Tamura, T. Furukawa, M. Neo, Y. Matsusue, Y. Shikinami, M. Okuno and T. Nakamura, *Biomaterials*, 2006, **27**, 1327–1332.
45 N. Ignjatović, V. Wu, Z. Ajduković, T. Mihajilov-Krstev, V. Uskoković and D. Uskoković, *Mater. Sci. Eng. C*, 2016, **60**, 357–364.
46 J. P. Bonjour, *J. Am. Coll. Nutr.*, 2011, **30**, 438S–448S.
47 J. Ahn, N. S. Kim, B. K. Lee, J. Park and Y. Kim, *J. Korean Med. Sci.*, 2018, **33**, e278–e278.
48 N. L. Ignjatović, C. Z. Liu, J. T. Czernuszka and D. P. Uskoković, *Acta Biomater.*, 2007, **3**, 927–935.
49 V. M. Rusu, C.-H. H. Ng, M. Wilke, B. Tiersch, P. Fratzl and M. G. Peter, *Biomaterials*, 2005, **26**, 5414–5426.
50 V. Uskoković, *J. Dispers. Sci. Technol*. 2012, **33**, 1762-1786.].
51 P. Paisrisarn, S. Tepaamorndech, M. Khongkow, P. Khemthong, P. Kasamechonchung, W. Klysubun, T. Wutikhun, L. Huang, K. Chantarasakha and S. Boonrungsiman, *Toxicol. Lett.*, 2018, **299**, 172–181.
52 H. Li, X. Guo and X. Ye, *J. Environ. Sci. (China)*, 2017, **52**, 141–150.
53 J. Wan, G. Zeng, D. Huang, L. Hu, P. Xu, C. Huang, R. Deng, W. Xue, C. Lai, C. Zhou, K. Zheng, X. Ren and X. Gong, *J. Hazard. Mater.*, 2018, **343**, 332–339.
54 Z. Yang, Z. Fang, P. E. Tsang, J. Fang and D. Zhao, *J. Environ. Manage.*, 2016, **182**, 247–251.
55 L. Wei, S. Wang, Q. Zuo, S. Liang, S. Shen and C. Zhao, *Environ. Sci. Process. Impacts*, 2016, **18**, 760–767.
56 J. D. Pasteris and B. Wopenka, *Mater. Sci. Eng. C*, 2005, **25**, 131–143.
57 C. Liu, L. Wang, J. Yin, L. Qi and Y. Feng, *Bull. Environ. Contam. Toxicol.*, 2018, **100**, 581–587.
58 R. Liu and D. Zhao, *Chemosphere*, 2013, **91**, 594–601.
59 S. Lee, J. An, Y. J. Kim and K. Nam, *J. Hazard. Mater.*, 2011, **186**, 2117–2122.
60 G. Flora, D. Gupta and A. Tiwari, *Interdiscip. Toxicol.*, 2012, **5**, 47–58.
61 G. F. Nordberg, *Toxicol. Lett.*, 2010, **192**, 45–49.
62 M. Andjelkovic, A. Buha Djordjevic, E. Antonijevic, B. Antonijevic, M. Stanic, J. Kotur-Stevuljevic, V. Spasojevic-Kalimanovska, M. Jovanovic, N. Boricic, D. Wallace and Z. Bulat, *Int. J. Environ. Res. Public Health*, 2019, **16**, 274.
63 H. I. Afridi, T. G. Kazi, F. N. Talpur and D. Brabazon, *Clin. Lab.*, 2015, **61**, 123–140.
64 L. Chang, S. Shen, Z. Zhang, X. Song and Q. Jiang, *Ann. Transl. Med.*, 2018, **6**, 320–320.
65 J. A. A. Brito, I. M. Costa, A. M. e Silva, J. M. S. Marques, C. M. Zagalo, I. I. B. Cavaleiro, T. A. P. Fernandes and L. L. Gonçalves, *Bone*, 2014, **64**, 228–234.
66 X. Chen, S. Ren, G. Zhu, Z. Wang and X. Wen, *Environ. Toxicol. Pharmacol.*, 2017, **54**, 162–168.
67 E. Tomaszewska, P. Dobrowolski, A. Winiarska-Mieczan, M. Kwiecień, S. Muszyński and A. Tomczyk, *Toxicol. Ind. Health*, 2017, **33**, 855–866.
68 K. Nambunmee, M. Nishijo, W. Swaddiwudhipong and W. Ruangyuttikarn, *J. Res. Heal. Sci.* 2018, **18**, 00419.
69 X. Cheng, Y. Niu, Q. Ding, X. Yin, G. Huang, J. Peng and J. Song, *Med. (United States)*, 2016, **95**, e2932–e2932.
70 H. D. Phuc, T. Kido, N. T. P. Oanh, H. D. Manh, L. T. Anh, Y. Oyama, R. Okamoto, A. Ichimori, K. Nogawa, Y. Suwazono and H. Nakagawa, *J. Appl. Toxicol.*, 2017, **37**, 1046–1052.
71 H. C. Gonick, *Indian J. Med. Res.*, 2008, **128**, 335–352.
72 J. B. Carey, A. Allshire and F. N. van Pelt, *Toxicol. Sci.*, 2006, **91**, 113–122.
73 M. Svartengren, C. G. Elinder, L. Friberg and B. Lind, *Environ. Res.*, 1986, **39**, 1–7.
74 H. W. Sun, D. J. Ma, C. Y. Chao, S. Liu and Z. B. Yuan, *Environ. Technol.*, 2009, **30**, 1051–1057.